Biogeosciences Discuss., doi:10.5194/bg-2017-73, 2017
Manuscript under review for journal Biogeosciences
Discussion started: 13 March 2017

Biogeosciences Discussions Open Access EGU

Nitrous oxide variability at sub-kilometre resolution in the Atlantic sector of the Southern Ocean

Imke Grefe[1,*], Sophie Fielding[2], Karen J. Heywood[1], Jan Kaiser[1]

[1]Centre for Ocean and Atmospheric Sciences, School of Environmental Sciences, University of East Anglia, NR4 7TJ Norwich, UK
[2] British Antarctic Survey, High Cross, Madingley Road, Cambridge, CB3 0ET, UK
[*]Now at: Lancaster Environment Centre, Lancaster University, LA1 4YQ Lancaster, UK

Correspondence to: Imke Grefe (i.grefe@lancaster.ac.uk), Jan Kaiser (j.kaiser@uea.ac.uk)

Abstract

The Southern Ocean is an important region for global nitrous oxide (N_2O) cycling. The contribution of different source and sink mechanisms is, however, not very well constrained due to a scarcity of seawater data from the area. Here we present high-resolution surface N_2O measurements from the Atlantic sector of the Southern Ocean, taking advantage of a relatively new underway setup allowing for collection of data during transit across mesoscale features such as frontal systems and eddies. Covering a range of different environments and biogeochemical settings, N_2O saturations and sea-to-air flux were highly variable: Saturations ranged from 96.5 % at the sea ice edge in the Weddell Sea to 126.1 % across the Polar Frontal Zone during transit to South Georgia. Negative sea-to-air fluxes of up to -1.3 µmol m^{-2} d^{-1} were observed in the Subantarctic Zone and highest positive fluxes of 14.5 µmol m^{-2} d^{-1} in Stromness Bay, coastal South Georgia.

1 Introduction

Nitrous oxide (N_2O) is a strong greenhouse gas and currently the third largest contributor to radiative forcing after carbon dioxide (CO_2) and methane (CH_4) (Hartmann et al., 2013). Furthermore, N_2O is an important source for stratospheric NO_x, which is involved in catalytic ozone depletion (Crutzen 1970; Ravishankara et al. 2009). The ocean, including coastal zones, estuaries and rivers, is estimated to contribute approximately 25 % to global N_2O emissions (Myhre et al., 2013). The Southern Ocean alone is estimated to account for 5 % of global emissions (0.9 Tg a^{-1} N (nitrogen equivalents), Nevison et al., 2005). However, measurements of oceanic N_2O concentrations in this region are scarce and these emission estimates are based on atmospheric measurements at Cape Grim and a few seawater measurements in the Southern Ocean from 1977-1993 (Nevison et al., 1995, 2004 and references therein).

The Scotia Sea in the Atlantic sector of the Southern Ocean is confined by the Scotia Ridge to the north, east and south and the Drake Passage to the west (Atkinson et al., 2001). South Georgia is part of the North Scotia Ridge in the path of the Antarctic Circumpolar Current (ACC) and within the Antarctic Zone (AAZ) south of the Polar Front (PF). Waters around South Georgia are characterised by high abundances of phytoplankton, zooplankton and vertebrate predators (Atkinson et al.,

2001), whereas most other areas of the Southern Ocean are dominated by High Nutrient Low Chlorophyll (HNLC) conditions (Martin, 1990). A relatively stable water column and benthic iron input support productivity in the vicinity of the island (Holeton et al., 2005; Korb et al., 2005).

To the south of the Scotia Sea the Weddell Sea is characterised by a large gyre, flowing eastwards until 20-30° E, returning westwards along the continental margin and following the eastern coast of the Antarctic Peninsula northwards (Deacon, 1979). Seasonal blooms in the Weddell Sea are associated with the Antarctic shelf and the ice edge (El-Sayed and Taguchi, 1981; Kristiansen et al., 1992; Nelson et al., 1989; Smith Jr and Nelson, 1990). Furthermore, drifting icebergs stimulate productivity by input of terrigenous iron through melt water (Biddle et al., 2015; Smith et al., 2007).

Generally, the Southern Ocean has the potential for both production and removal of N_2O (Rees et al., 1997): Solubility of N_2O increases at lower temperatures, and together with downwelling areas associated with deep-water formation and convergences in the Antarctic frontal zones, wide areas could function as sinks. On the other hand, upwelling of deep and intermediate waters could be a source of biologically produced N_2O to the atmosphere. Artificial iron fertilisation of the Southern Ocean may stimulate biological CO_2 uptake, but could potentially increase N_2O production, offsetting the benefits of CO_2 sequestration in terms of radiative forcing (Fuhrman and Capone, 1991; Jin and Gruber, 2003). While an iron fertilisation experiment in the Australasian sector of the Southern Ocean showed N_2O accumulation in the pycnocline (Law and Ling, 2001), no increase in N_2O concentrations was observed during a similar experiment in the Atlantic subpolar sector (Walter et al., 2005).

Here, we present high-resolution measurements of ocean surface N_2O concentrations from the Scotia Sea and Weddell Sea. Using off-axis Integrated Cavity Output Spectroscopy (ICOS) (Arevalo-Martinez et al., 2013; Grefe and Kaiser, 2014) combined with wind-speed gas exchange parameterisations we can resolve small-scale variability in N_2O fluxes and capture the impact of frontal structures and changes in weather conditions on emissions from the Southern Ocean.

2 Methods

N_2O concentrations in surface waters were measured during the annual Western Core Box (WCB) krill survey in the Scotia Sea between 28 December 2011 and 16 January 2012 (JR260B) and in the Weddell Sea from 20 January to 2 February 2012 (JR255A/GENTOO Gliders: Excellent New Tools for Observing the Ocean) on board RRS *James Clark Ross*. The measurement region for both cruises is shown in Fig. 1.

The setup and performance of the coupled analyser-equilibrator system is described in Grefe and Kaiser (2014). Briefly, a percolating glass bed equilibrator was connected to a N_2O/CO analyser (N_2O/CO-23d, Los Gatos Research Inc.). Artificial air mixtures (21 % O_2, 79 % N_2) with nominal N_2O mole fractions of 300, 320 and 340 nmol mol^{-1} (BOC) were used as reference gases. These gas mixtures were compared with IMECC/NOAA standards to determine the exact values of (297.6±0.1), (325.3±0.1) and (344.2±0.1) nmol mol^{-1} (NOAA-2006 scale). Reference gases and marine background air were

Biogeosciences Discuss., doi:10.5194/bg-2017-73, 2017
Manuscript under review for journal Biogeosciences
Discussion started: 13 March 2017

measured twice a day for 20 min each during JR260B. Due to sufficient analyser stability during this cruise, calibration was reduced to once a day during JR255A/GENTOO. To ensure complete flushing of the cavity, only the last 5 min of each 20-min gas measurement were evaluated. Correspondingly, the first 15 min of equilibrator data following the reference gas and air measurements were discarded. Precision for single reference measurements (standard deviation of measurements at 1Hz over 5 min) was 0.4 nmol mol^{-1}. The standard deviation of the uncorrected reference gas measurements throughout JR260B was 1.1 nmol mol^{-1} (n = 29) and 0.8 nmol mol^{-1} (n = 19) for JR255A/GENTOO. To estimate the long-term repeatability of the measurements after calibration, we used the standards with the lowest and highest N_2O mole fraction to calibrate the standard with the middle N_2O mole fraction. The mean difference between resulting calibrated N_2O mole fraction and the actual value of 325.3 nmol mol^{-1} was (0.2±0.1) nmol mol^{-1}, corresponding to a precision better than 0.1 %. The flow rate of the headspace gas through the analyser was 400 mL min^{-1} (293 K, 1 bar) resulting in a 95 % relaxation time (t_{95} = 3τ) of approximately 7 minutes (Grefe and Kaiser, 2014). Data was acquired at a rate of 1 Hz; which was binned into 60 s averages for data evaluation purposes. Water flow through the equilibrator was held constant at 1.8-1.9 L min^{-1}, using a flow regulator (Robert Pearson & Company Ltd, ½ inch diameter tap tail flow regulator). Water temperature in the equilibrator was measured with a Pt-100 temperature probe (Omega Engineering Limited), calibrated against a mercury reference thermometer to within ±0.06 ºC, and recorded using a RTD temperature recorder and USB Datalogger interface (both Omega Engineering Limited).

3 Results and discussion

3.1 N_2O concentrations and saturations in the surface ocean

Concentration of dissolved N_2O (c) was calculated from the dry mole fraction measured in the equilibrator headspace (x), water temperature in the equilibrator (T_{eq}), salinity (S) and atmospheric pressure (p_{air}) using the solubility function F as described by Weiss and Price (1980), Eq. (1).

$$c = xF(T_{eq}, S)p_{air}\ , \quad (1)$$

N_2O saturation in surface waters (s) was calculated by comparing x with the atmospheric mole fraction x_{air} and the respective equilibrium concentrations for (T_{eq}) and temperature at the seawater intake (T_{in}) Eq. (2).

$$s = \frac{xF(T_{eq},S)}{x_{air}F(T_{in},S)} \quad (2)$$

Values for p_{air}, S and T_{in} were from the ship's surface water and meteorological monitoring system Surfmet (http://www.bodc.ac.uk).

N_2O dry mole fractions measured in marine air were on average (323.6±0.6) nmol mol^{-1} during JR260B and (324.0±0.7) during JR255A/GENTOO. These values agree within measurement uncertainties with data from the Advanced Global

Biogeosciences Discuss., doi:10.5194/bg-2017-73, 2017
Manuscript under review for journal Biogeosciences
Discussion started: 13 March 2017

Atmospheric Gases Experiment (AGAGE) for Cape Grim, Tasmania in January 2012 (40.68° S 144.69° E, (323.9±0.5) nmol mol^{-1}).

3.1.1 JR160B

Concentrations and saturations of N_2O in the surface ocean for JR260B are shown in Fig. 2a and b, respectively. The average N_2O concentration was (14.0±0.7) nmol L^{-1}, with lowest values of 11.2 nmol L^{-1} near the Falkland Islands and highest values of 16.2 nmol L^{-1} while crossing the Polar Frontal Zone (PFZ) during transit to South Georgia.

The average N_2O saturation was (104.3±3.4) %. Lowest saturations of 99.4 % were observed in the Subantarctic Zone (SAZ) during transit from South Georgia back to the Falkland Islands. Saturations were highest to the east of the PF (126.1 %) where surface concentrations were also highest.

Subantarctic Zone SAZ

In the Subantarctic Surface Waters (SASW) close to the Falkland Islands to the east of the Subantarctic Front (SAF), average surface concentrations were low, while saturations were similar to those observed in the Antarctic Zone (AAZ) (11.4±0.2) nmol L^{-1}, (102.4±0.7) %, see below). Water temperature and salinity were higher than the Antarctic waters south and east of the PF, so the difference in concentrations was likely due to solubility effects. The Falkland current transports nutrient-rich waters from the ACC onto the Falkland shelf (Peterson and Whitworth, 1989), potentially supporting N_2O production during remineralisation in the SAZ.

Polar Frontal Zone PFZ

N_2O concentrations across the PFZ between the SAF and PF were highly variable with values ranging from 11.4 to 16.2 nmol L^{-1} (101.7 to 126.1 % saturation) while water temperature and salinity were decreasing towards the east. Average concentrations and saturations across the PFZ were (13.8±0.9) nmol L^{-1} and (108.8±5.2) %, respectively.

The most important sources of N_2O to surface waters are upwelling of old water masses with preformed high N_2O concentrations and in situ production during remineralisation or denitrification. High N_2O saturations across the PFZ could neither be attributed to a specific water mass, nor to a point on the mixing line between Subantarctic Surface Water (SASW) and Antarctic Surface Water (AASW) (Fig. 3).

Frontal systems can supply nutrients and iron to surface waters with large phytoplankton blooms forming across the PFZ, potentially fuelled by iron input from the Antarctic Peninsula archipelago, the Scotia Ridge and Georgia Rise (de Baar et al., 1995). Re-mineralisation of sinking bloom-biomass could lead to enhanced in situ N_2O production across the PFZ, resulting in the high saturations values observed during JR260B.

Antarctic Zone AAZ

Average N_2O concentrations in the Antarctic Zone (AAZ) to the west of the PF near South Georgia were substantially higher than in the SAZ (14.1±0.4) nmol L^{-1}. Saturations, however, were only slightly increased ((103.9±3.1) %), similar to values of (103.0±2.0)% previously observed in the region (Weiss et al., 1992). The lower water temperature and salinity of Antarctic Surface Water AASW increased N_2O solubility, resulting in lower saturation values. Upwelling of deep water masses would not be expected away from the ACC and denitrification is not likely to take place in the oxygenated surface waters of the AAZ. Nitrification and nitrifier-denitrification would be more likely sources of in situ N_2O production. High nitrification rates (> 30 mmol m^{-2} d^{-1}) were suggested for the Pacific sector of the Southern Ocean south of the PF (Sambrotto and Mace, 2000) and could also account for N_2O supersaturation observed in the AAZ of the Atlantic sector. Extensive phytoplankton blooms were observed in the vicinity of South Georgia and across the Scotia Sea, extending to the southern limit of the Polar Front (Korb et al., 2004, 2005). These blooms can develop due to a stable water column over the shelf and iron input from the shelf sediments and island runoff (de Baar et al., 1995; Holeton et al., 2005; Korb et al., 2005; Wadley et al., 2014). This accumulation of biomass would supply ample substrate to sustain high nitrification rates and N_2O production could lead to the observed supersaturating close to the island. Not much is known about nitrifier-denitrification in polar waters, additional research is required to estimate the importance of this production pathway for N_2O accumulations in surface waters.

Stromness Bay

N_2O concentrations and saturations in coastal Stromness Bay, South Georgia, were higher than in the open waters of the AAZ ((14.8±0.3) nmol L^{-1} and (108.1±2.6) %, respectively) with highest saturations observed where fresh meltwater runoff from the island was mixing with AASW (Fig. 3). Terrestrial runoff can transport iron and biomass from land into the sea and stimulate productivity and subsequent remineralisation where N_2O is produced during nitrification. In addition, fur seals (*Arctocephalus gazella*) and macaroni penguins (*Eudyptes chrysolophus*) have large breeding colonies on South Georgia, re-distributing nitrogen from their hunting grounds to the island (Whitehouse et al., 1999). The high nitrogen load in coastal waters is expected to lead to high N_2O saturations (Bange et al., 1996). Nitrifier-denitrification in anoxic sites of suspended particles can be an additional source of N_2O (Ostrom et al., 2000). As the water depth in Stromness Bay is shallow (60 m) and well mixed at the anchoring site, N_2O produced by denitrification at the sediment interface could have diffused into the water column, contributing to the high concentration at the surface.

3.1.2 JR255A/GENTOO

During JR255A/GENTOO, average N_2O surface concentrations were (14.9±1.2) nmol L^{-1}, corresponding to saturations of (103.1±3.6) %. While N_2O concentrations were higher than for JR260B, mainly due to the lower water temperatures, average saturations were slightly lower. Lowest N_2O surface concentrations of 10.6 nmol L^{-1} were observed on the South American shelf close to the Falkland Islands (Fig. 4a). Concentrations and saturations were highest across the South Scotia Ridge (up to 17.0 nmol L^{-1}, corresponding to 116.0 % saturation, Fig. 4b). The lowest saturations were observed close to the sea ice edge in the open waters of the Weddell Sea (96.5 %).

Biogeosciences Discuss., doi:10.5194/bg-2017-73, 2017
Manuscript under review for journal Biogeosciences
Discussion started: 13 March 2017

Drake Passage

Average N_2O concentrations at the beginning of the cruise were (13.7±1.8) nmol L^{-1} ((102.9±4.2) % saturation). Decreasing temperatures during transit across Drake Passage to the Eastern Antarctic Peninsula partially accounted for increasing N_2O concentrations (Fig. 4a), resulting in a wide range of concentration values across the region, whereas saturations were on average only slightly above equilibrium with the atmosphere. Water masses across Drake Passage were Subantarctic Surface Water to the north of the SAF and Antarctic Surface Water to the south of the PF (SASW and AASW, respectively) (Fig. 5). These surface waters are in constant contact with the atmosphere and are expected to be in equilibrium with the atmosphere in absence of biological N_2O sources. N_2O saturations above 100 % could be due to in situ production during remineralisation of biomass. For comparison, Rees et al. (1997) observed slightly lower saturations for Drake Passage ((99.7±3.0)%), while Weiss et al. (1992) reported values close to the data presented here (Ajax 2: (102.3±0.9)%, JR255A/GENTOO: (102.9±4.2)%). Higher saturation values for Weiss et al. (1992) and JR255A/GENTOO could be due to interannual and seasonal variability. JR255A/GENTOO and Ajax 2 took place in January and February, later in the austral summer season than the November/December cruise of Rees et al. (1997). Nitrification as part of the remineralisation of sinking biomass could have increased N_2O accumulations in the surface over the summer, resulting in higher values later in the growing season.

Just south of the Southern Boundary of the Antarctic Circumpolar Current (SB), concentrations, as well as saturations, reached the highest values observed during JR255A/GENTOO. Temperature and salinity characteristics of the surface water indicated an influence of Upper Circumpolar Deep Water (UCDW) from below (Fig. 5, Orsi et al., 1995). UCDW is an old water mass, high in remineralised nutrients and N_2O as a byproduct of nitrification. Iron input from the Scotia Ridge, as observed by Klunder et al. (2014) could additionally enhance productivity, supplying substrate in form of sinking particles for in situ N_2O production.

Weddell Sea

Surface N_2O concentrations of the open waters of the Weddell Sea were on average (15.2±0.2) nmol L^{-1} ((102.2±1.6) % saturation). South of the ACC, the surface waters were colder than across Drake Passage, increasing the solubility of N_2O and resulting in slightly lower saturations despite higher concentrations.

Higher-than-average N_2O saturations were observed on the Antarctic shelf off the tip of Joinville Island ((104.2±1.7) %) and during the section across the large standing eddy forming over the South Scotia Ridge, centred on 62° S and 54° W (Thompson et al., 2009) ((110.5±1.2) %) (Fig. 4a and b). Iron from the sediments, as well as land run-off could have stimulated productivity in these areas (Klunder et al., 2014; Sañudo-Wilhelmy et al., 2002). In addition, the sampling region was more sheltered from the circumpolar winds by the Antarctic Peninsula, stabilising the water column over the shallow bathymetry. The combination of ample supply of trace nutrients and a stable water column, keeping phototrophic organisms

Biogeosciences Discuss., doi:10.5194/bg-2017-73, 2017
Manuscript under review for journal Biogeosciences
Discussion started: 13 March 2017

in the euphotic zone, presumably resulted in comparably high productivity and subsequent N_2O production during remineralisation of sinking biomass.

Sea ice edge

Lowest saturations of on average (98.8.0±1.3) % were observed close to the sea ice edge in the south east of the survey region (Fig. 4b). N_2O concentrations were similar to other open ocean regions in the Weddell Sea ((15.4±0.2) nmol L^{-1} at the ice edge compared to (15.2±0.2) nmol L^{-1}). Saturations, however, were lower due to lower temperature and salinity, resulting in higher N_2O solubility. Randall et al. (2012) observed under-saturations of N_2O within sea ice due to loss of dissolved gases during brine rejection. Mixing of seawater with under-saturated melt water would decrease surface concentrations, which was not observed during JR255A. However, it is possible that end-members were not captured in these measurements and the mixing line for temperature and salinity indeed indicates dilution of Weddell Sea surface waters with melt water low in N_2O.

3.2 N_2O sea-to-air flux

Sea-to-air flux was calculated using wind speeds from the CCMP Wind Vector Analysis Product (www.remss.com/measurements/ccmp). The gas transfer coefficient (k_w) was calculated, using the parameterisation of Nightingale (2000) (Equation 3) and k_w was adjusted for N_2O with the Schmidt number *Sc* calculated following (Wanninkhof, 1992), Eq. (3).

$$\frac{k_w}{\mathrm{m\ d^{-1}}} = 0.24\left[0.222\left(\frac{u_{CCMP}}{\mathrm{m\ s^{-1}}}\right)^2 + 0.333\frac{u_{CCMP}}{\mathrm{m\ s^{-1}}}\right]\left(\frac{Sc}{600}\right)^{-0.5} \quad (3)$$

The air-sea flux (Φ) was calculated from k_w and the difference between N_2O concentrations in seawater *c* and air saturation concentrations (c_{sat}), Eq. (4):

$$\Phi = k_w(c - c_{air}) = k_w\left[c - x_{air}\frac{u_{CCMP}}{\mathrm{m\ s^{-1}}}\right]\left(\frac{Sc}{600}\right)^{-0.5} \quad (4)$$

3.2.1 JR160B

Surface waters during JR260B were mainly a source of N_2O to the atmosphere (Fig. 6). The average flux of 2.3 µmol m^{-2} d^{-1} was higher than the global average flux of 1.1 µmol m^{-2} d^{-1} (based on a marine contribution of 25 % to global N_2O emissions (Ciais et al., 2013)).

The average sea-to-air flux within the SAZ was ((1.1±0.4) µmol m^{-2} d^{-1}), due to low to moderate wind speeds at the time of measurements and saturations just slightly above equilibrium with the atmosphere.

N_2O flux was increasing across the PFZ to an average of (3.6±2.4) µmol m^{-2} d^{-1} with highest values of 13.3 µmol m^{-2} d^{-1} during transit from South Georgia back to the Falkland Islands. Average global flux values were highly exceeded across the

frontal zone as high N_2O supersaturations, possibly a result of in situ production due to high biomass supported by iron supply from sediments, coincide with high circumpolar wind speeds.

Sea-to-air flux decreased again in the open waters of the AAZ around South Georgia as N_2O supersaturations were lower. The average flux of (1.8±1.8) µmol m^{-2} d^{-1} was, however, still exceeding the global average. Negative flux up to -0.5 µmol m^{-2} d^{-1} was only observed briefly to the east of the PF during transit to South Georgia.

In contrast to the open waters of the AAZ, Stromness Bay was a strong source of N_2O to the atmosphere while the ship was anchored for calibration of acoustic instruments. Sea-to-air flux was initially only slightly higher than for the surrounding open ocean area (2.2 µmol m^{-2} d^{-1}), despite high N_2O supersaturations in the bay. This was due to low wind speeds of 7.3 m s^{-1}, which subsequently increased to 14.5 m s^{-1} throughout the day, resulting in sea-to-air fluxes of up to 10.6 µmol m^{-2} d^{-1} and an average of (4.5±2.4) µmol m^{-2} d^{-1}.

Overall, the surface ocean was a strong source of N_2O to the atmosphere for most of the research cruise JR260B with sea-to-air fluxes exceeding global average flux. These high flux rates were driven by high surface water saturations, presumably resulting from in situ production, and moderate to high wind speed.

3.2.2 JR255A/GENTOO

The average sea-to-air N_2O flux throughout JR255A/GENTOO was (0.7±0.9) µmol m^{-2} d^{-1}, which is below global average values of 1.1 µmol m^{-2} d^{-1} and considerably lower than the average flux for JR260B, just to the north of the JR255A/GENTOO region. The low flux was a result of lower saturation values compared with JR260B, but still above equilibrium with the atmosphere for most of the cruise. Additionally, wind speeds were lower during JR255A/GENTOO.

Highest sea-to-air flux of 6.8 µmol m^{-2} d^{-1} was observed across the South Scotia Ridge where high wind speeds coincided with high N_2O supersaturations, presumably due to surface waters being influenced by underlying UCDW high in N_2O.

Although surface waters were most strongly undersaturated at the sea ice edge, negative fluxes were highest at the beginning of the cruise, close to the Falkland Islands (-1.3 µmol m^{-2} d^{-1}). Highest wind speeds of up to 13.3. m s^{-1} were observed at the beginning of the cruise, driving the strong negative fluxes on the shelf. At the ice edge, in contrast, wind speeds were considerably lower (1.4 to 6 m s^{-1}), resulting in weaker negative fluxes.

Low wind speeds also affected sea-to-air flux on the Antarctic shelf close to Joinville Island, as well as across the standing eddy over the South Scotia Ridge. Despite relatively high supersaturations, N_2O flux was rather low ((0.5±0.2) and (0.5±0.4) µmol m^{-2} d^{-1}, respectively).

Throughout JR255A sea-to-air flux of N_2O was low compared to JR260B and the global average, mainly due to low wind speed rather than low N_2O saturation of surface waters. Areas like the continental shelf, eddies and the ice edge hold the potential for substantial N_2O sources and sinks if wind speed increases and production in the water column is sustained.

Biogeosciences Discuss., doi:10.5194/bg-2017-73, 2017
Manuscript under review for journal Biogeosciences
Discussion started: 13 March 2017

Summary

For both cruises, JR260B and JR255A/GENTOO, high N_2O saturations were observed over shallow bathymetry across the North and South Scotia Ridge and on the Antarctic shelf and coastal South Georgia. This might be due to iron input supporting biomass production, which then forms the substrate for N_2O production (Fuhrman and Capone, 1991; Jin and Gruber, 2003).

Frontal systems represented another source region for N_2O. To the east of Drake Passage during JR260B, high N_2O saturations across the PFZ were presumably the result of in situ production during remineralisation of sinking biomass. South of Drake Passage across the South Scotia Ridge/south of the SB during JR255A UCDW influencing surface waters resulted in a strong source of N_2O to the atmosphere. The frontal system of the ACC can be an important source of N_2O, but the observed supersaturation was highly variable. High-resolution measurements are a valuable tool for accurately assessing N_2O emissions from this region.

Assuming that the average flux values of 2.3 µmol m^{-2} d^{-1} and 0.7 µmol m^{-2} d^{-1} calculated for JR260B and JR255A are representative for the Scotia Sea and Weddell Sea over time, the combined area could contribute 0.04 Tg a^{-1} N (nitrogen equivalent) to the global N_2O source. While this value is relatively low, also compared to model estimates of 0.9 Tg a^{-1} N (nitrogen equivalents) for the entire Southern Ocean (Nevison et al., 2005), areas with a strong variability in N_2O saturation and sea-to-air flux were observed for both cruises. These findings indicate the importance of high-resolution data to accurately estimate the source strength of mesoscale features, such as frontal systems and eddies.

Competing interests: The authors declare that they have no conflict of interest.

Acknowledgements

We would like to thank the officers and crew on board RRS James Clark Ross and the scientific party for their support during JR260B and JR255A/GENTOO. We also thank Sunke Schmidtko for supplying calibrated sea surface temperature and salinity, Dorothee Bakker for providing the equilibrator used in this study and Gareth A. Lee for technical support. This study was supported by the European Community's Seventh Framework Programme (FP7/2007-2013) under grant agreement number 237890 (Marie Curie Initial Training Network "INTRAMIF") and the NERC Collaborative Gearing Scheme, project number AFI CGS78. We acknowledge the BAS Ecosystems Long Term Monitoring and Survey Programme Western Core Box (LTMS WCB).

References

Arevalo-Martinez, D. L., Beiyer, M., Krumbholz, M., Piller, I., Kock, A., Steinhof, T., Körtzinger, A. and Bange, H. W.: A

new method for continuous measurements of oceanic and atmospheric N_2O, CO and CO_2: Performance of off-axis integrated cavity output spectroscopy (OA-ICOS) coupled to non-dispersive infrared detection (NDIR), Ocean Sci., 9(6), 1071–1087, 2013.

Atkinson, A., Whitehouse, M. J., Priddle, J., Cripps, G. C., Ward, P. and Brandon, M. A.: South Georgia, Antarctica: a productive, cold water, pelagic ecosystem, Mar. Ecol. Prog. Ser., (216), 279–308, 2001.

de Baar, H. J. W., de Jong, J. T. M., Bakker, D. C. E., Löscher, B. M., Veth, C., Bathmann, U. and Smetacek, V.: Importance of iron for plankton blooms and carbon dioxide drawdown in the Southern Ocean, Nature, 373, 412–415, doi:10.1038/373412a0, 1995.

Bange, H., Rapsomanikis, S. and Andreae, M.: Nitrous oxide in coastal waters, Global Biogeochem. Cycles, 10(1), 197–207, doi:10.1029/95GB03834, 1996.

Biddle, L. C., Kaiser, J., Heywood, K. J., Thompson, A. F. and Jenkins, A.: Ocean glider observations of iceberg-enhanced biological production in the northwestern Weddell Sea, Geophys. Res. Lett., 42(2), 459–465, doi:10.1002/2014GL062850, 2015.

Ciais, P., Sabine, C., Bala, G., Bopp, L., Brovkin, V., Canadell, J., Chhabra, A., DeFries, R., Galloway, J., Heimann, M., Jones, C., Le Quéré, C., Myneni, R. B., Thornton, S. and Piao, P.: Carbon and Other Biogeochemical Cycles, in Climate Change 2013: The Physical Science Basis. Contribution of Working Group I to the Fifth Assessment Report of the Intergovernmental Panel on Climate Change, edited by T. F. Stocker, D. Qin, G.-K. Plattner, M. Tignor, S. K. Allen, J. Boschung, A. Nauels, Y. Xia, V. Bex, and P. M. Midgley, Cambridge University Press, Cambridge, United Kingdom and New York, NY, USA., 2013.

Crutzen, P. J.: The influence of nitrogen oxides on the atmospheric ozone content, Q. J. R. Meteorol. Soc., 320–325, 1970.

Deacon, G. E. R.: The Weddell gyre, Deep Sea Res. Part A, Oceanogr. Res. Pap., 26(9), 981–995, doi:10.1016/0198-0149(79)90044-X, 1979.

El-Sayed, S. Z. and Taguchi, S.: Primary production and standing crop of phytoplankton along the ice-edge in the Weddell Sea, Deep Sea Res. Part A, Oceanogr. Res. Pap., 28(9), 1017–1032, doi:10.1016/0198-0149(81)90015-7, 1981.

Fuhrman, J. A. and Capone, D. G.: Possible biogeochemical consequences of ocean fertilization, Limnol. Oceanogr., 36, 1951–1959, doi:10.4319/lo.1991.36.8.1951, 1991.

Grefe, I. and Kaiser, J.: Equilibrator-based measurements of dissolved nitrous oxide in the surface ocean using an integrated cavity output laser absorption spectrometer, Ocean Sci., 10(3), 501–512, doi:10.5194/os-10-501-2014, 2014.

Hartmann, D. L., Klein Tank, A. M. G., Rusticucci, M., Alexander, L. V., Brönnimann, S., Charabi, Y., Dentener, F. J., Dlugokencky, E. J., Easterling, D. R., Kaplan, A., Soden, B. J., Thorne, P. W., Wild, M. and Zhai, P. M.: Observations:

Atmosphere and Surface. In: Climate Change 2013: The Physical Science Basis. Contribution of Working Group I to the Fifth Assessment Report of the Intergovernmental Panel on Climate Change, edited by T. F. Stocker, D. Qin, G.-K. Plattner, M. Tignor, S. K. Allen, J. Boschung, A. Nauels, Y. Xia, V. Bex, and P. M. Midgley, Cambridge University Press., 2013.

Holeton, C. L., Nédélec, F., Sanders, R., Brown, L., Moore, C. M., Stevens, D. P., Heywood, K. J., Statham, P. J. and Lucas, C. H.: Physiological state of phytoplankton communities in the Southwest Atlantic sector of the Southern Ocean, as measured by fast repetition rate fluorometry, Polar Biol., 29(1), 44–52, doi:10.1007/s00300-005-0028-y, 2005.

Jin, X. and Gruber, N.: Offsetting the radiative benefit of ocean iron fertilization by enhancing N_2O emissions, Geophys. Res. Lett., 30, 2249, doi:10.1029/2003GL018458, 2003.

Klunder, M. B., Laan, P., De Baar, H. J. W., Middag, R., Neven, I. and Van Ooijen, J.: Dissolved Fe across the Weddell Sea and Drake Passage: Impact of DFe on nutrient uptake, Biogeosciences, 11(3), 651–669, doi:10.5194/bg-11-651-2014, 2014.

Korb, R. E., Whitehouse, M. J. and Ward, P.: SeaWiFS in the southern ocean: spatial and temporal variability in phytoplankton biomass around South Georgia, Deep Sea Res. Part II Top. Stud. Oceanogr., 51(1-3), 99, doi:10.1016/j.dsr2.2003.04.002, 2004.

Korb, R. E., Whitehouse, M. J., Thorpe, S. E. and Gordon, M.: Primary production across the Scotia Sea in relation to the physico-chemical environment, J. Mar. Syst., 57(3-4), 231–249, doi:10.1016/j.jmarsys.2005.04.009, 2005.

Kristiansen, S., Syvertsen, E. E. and Farbrot, T.: Nitrogen Uptake in the Weddell Sea during Late Winter and Spring, Polar Biol., 12(2), 245–251, doi:10.1007/BF00238266, 1992.

Law, C. S. and Ling, R. D.: Nitrous oxide flux and response to increased iron availability in the Antarctic Circumpolar Current, Deep. Res. Part II: Topical Studies in Oceanography, 48(11), 2001.

Martin, J. H.: Glacial-Interglacial CO_2 changes: The Iron Hypothesis, Paleoceanography, 5(1), 1–13, doi:doi:10.1029/PA005i001p00001, 1990.

Myhre, G., Shindell, D., Bréon, F.-M., Collins, W., Fuglestvedt, J., Huang, J., Koch, D., Lamarque, J.-F., Lee, D., Mendoza, B., Nakajima, T., Robock, A., Stephens, G., Takemura, T. and Zhang, H.: Anthropogenic and Natural Radiative Forcing, in Climate Change 2013: The Physical Science Basis. Contribution of Working Group I to the Fifth Assessment Report of the Intergovernmental Panel on Climate Change, edited by V. B. and P. M. M. Stocker, T.F., D. Qin, G.-K. Plattner, M. Tignor, S.K. Allen, J. Boschung, A. Nauels, Y. Xia, Cambridge University Press, Cambridge, United Kingdom and New York, NY, USA., 2013.

Nelson, D. M., Smith, W. O., Muench, R. D., Gordon, L. I., Sullivan, C. W. and Husby, D. M.: Particulate matter and nutrient distributions in the ice-edge zone of the Weddell Sea: relationship to hydrography during late summer, Deep Sea Res. Part A, Oceanogr. Res. Pap., 36(2), 191–209, doi:10.1016/0198-0149(89)90133-7, 1989.

Nevison, C. D., Weiss, R. F. and J, E. D.: Global Oceanic Emissions of Nitrous-Oxide, J. Geophys. Res., 100(C8), 15809–15820, doi:10.1029/95JC00684, 1995.

Nevison, C. D., Lueker, T. J. and Weiss, R. F.: Quantifying the nitrous oxide source from coastal upwelling, Global Biogeochem. Cycles, 18(1), n/a–n/a, doi:10.1029/2003GB002110, 2004.

Nevison, C. D., Keeling, R. F., Weiss, R. F., Popp, B. N., Jin, X., Fraser, P. J., Porter, L. W. and Hess, P. G.: Southern Ocean ventilation inferred from seasonal cycles of atmospehric N_2O and O_2/N_2 at Cape Grim, Tasmania, Tellus, Ser. B Chem. Phys. Meteorol., 57(3), 218–229, doi:10.1111/j.1600-0889.2005.00143.x, 2005.

Nightingale, P. D., Malin, G., Law, C. S., Watson, A. J., Liss, P. S., Liddicoat, M. I., Boutin, J. and Upstill-Goddard, R. C.: In situ evaluation of air-sea gas exchange parameterizations using novel conservative and volatile tracers, Global Biogeochem. Cycles, 14(1), 373–387, 2000.

Orsi, A. H., Whitworth, T., and Nowlin, W. D.: On the meridional extent and fronts of the Antarctic Circumpolar Current, Deep Sea Research Part I: Oceanographic Research Papers, 45(5), 641-673, 1995.

Ostrom, N. E., Russ, M. E., Popp, B., Rust, T. M. and Karl, D. M.: Mechanisms of nitrous oxide production in the subtropical North Pacific based on determinations of the isotopic abundances of nitrous oxide and di-oxygen, Chemosph. - Glob. Chang. Sci., 2(3-4), 281–290, doi:10.1016/S1465-9972(00)00031-3, 2000.

Peterson, R. G. and Whitworth, T.: The Subantarctic and Polar Fronts in relation to deep water masses through the southwestern Atlantic, J. Geophys. Res. Ocean., 94(C8), 10817–10838, 1989.

Randall, K., Scarratt, M., Levasseur, M., Michaud, S., Xie, H. and Gosselin, M.: First measurements of nitrous oxide in Arctic sea ice, J. Geophys. Res., 117(C9), C00G15, doi:10.1029/2011jc007340, 2012.

Ravishankara, A. R., Daniel, J. S. and Portmann, R. W.: Nitrous oxide (N_2O): the dominant ozone-depleting substance emitted in the 21st century, Science 326(5949), 123–125, doi:10.1126/science.1176985, 2009.

Rees, A. P., Owens, N. J. P. and Upstill-Goddard, R. C.: Nitrous oxide in the Bellingshausen Sea and Drake Passage, J. Geophys. Res. Ocean., 102.C2, 3383–3391, 1997.

Sambrotto, R. N. and Mace, B. J.: Coupling of biological and physical regimes across the Antarctic Polar Front as reflected by nitrogen production and recycling, Deep. Res. Part II Top. Stud. Oceanogr., 47(15-16), 3339–3367, doi:10.1016/S0967-0645(00)00071-0, 2000.

Sañudo-Wilhelmy, S. A., Olsen, K. A., Scelfo, J. M., Foster, T. D. and Flegal, A. R.: Trace metal distributions off the antarctic peninsula in the weddell sea, Mar. Chem., 77(2-3), 157–170, doi:10.1016/S0304-4203(01)00084-6, 2002.

Smith Jr, W. O. and Nelson, D. M.: Phytoplankton growth and new production in the Weddell Sea marginal ice zone in the austral spring and autumn, Limnol. Oceanogr., 35(4), 809–821, doi:10.4319/lo.1990.35.4.0809, 1990.

Smith, K. L., Robison, B. H., Helly, J. J., Kaufmann, R. S., Ruhl, H. a, Shaw, T. J., Twining, B. S. and Vernet, M.: Free-drifting icebergs: hot spots of chemical and biological enrichment in the Weddell Sea, Science, 317(5837), 478–482, doi:10.1126/science.1142834, 2007.

Thompson, A. F., Heywood, K. J., Thorpe, S. E., Renner, A. H. H. and Trasviña, A.: Surface Circulation at the Tip of the Antarctic Peninsula from Drifters, J. Phys. Oceanogr., 39(1), 3–26, doi:10.1175/2008JPO3995.1, 2009.

Wadley, M. R., Jickells, T. D., Heywood, K. J.: The role of iron sources and transport for Southern Ocean productivity, Deep Sea Research Part I: Oceanographic Research Papers, 87, 82-94, 2014.

Walter, S., Peeken, I., Lochte, K., Webb, A. and Bange, H. W.: Nitrous oxide measurements during EIFEX, the European Iron Fertilization Experiment in the subpolar South Atlantic Ocean, Geophys. Res. Lett., 32, L23613, doi:10.1029/2005GL024619, 2005.

Wanninkhof, R.: Relationship Between Wind Speed and Gas Exchange, 97(92), 7373–7382, 1992.

Weiss, R. F., and Price, B. A.: Nitrous oxide solubility in water and seawater, Marine Chemistry 8.4, 347-359, 1980.

Weiss, R. F., Woy, F. A. Van, Salameh, P. K. and Sepanski, R. J.: Surface water and atmospheric carbon dioxide and nitrous oxide observations by shipboard automated gas chromatography: Results from expeditions between 1977 and 1990, 1992.

Whitehouse, M. J., Priddle, J., Brandon, M. A. and Swanson, C.: A comparison of chlorophyll/nutrient dynamics at two survey sites near South Georgia, and the potential role of planktonic nitrogen recycled by land-based predators, Limnol. Oceanogr., 44(6), 1498–1508, doi:10.4319/lo.1999.44.6.1498, 1999.

Biogeosciences Discuss., doi:10.5194/bg-2017-73, 2017
Manuscript under review for journal Biogeosciences
Discussion started: 13 March 2017

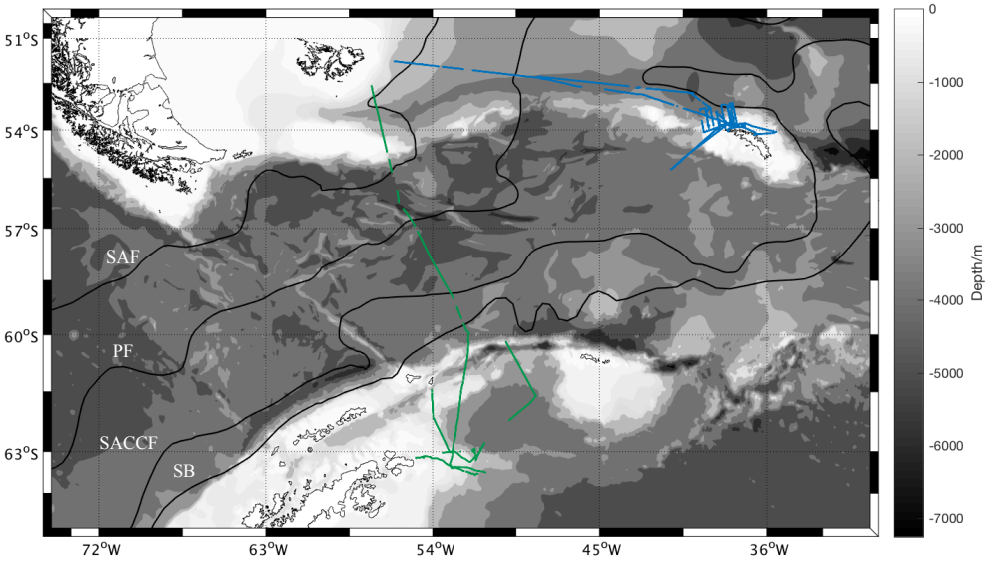

Figure 1: Sampling area with bathymetry from the General Bathymetric Chart of the Oceans (GEBCO) one minute grid. Isobaths every 1000 m between 8000 m and 1000 m depth, every 200 m between 1000 m and 0 m. N_2O measurement positions during JR260B in blue, N_2O measurement positions during JR255A/GENTOO in green. Climatological locations of fronts in black after Orsi et al. (1995).

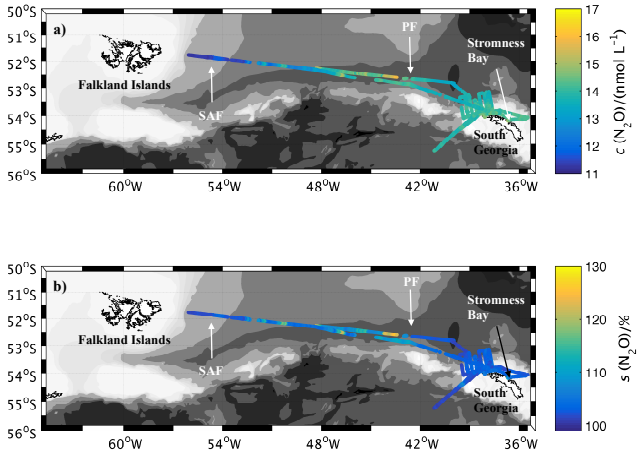

5

Biogeosciences Discuss., doi:10.5194/bg-2017-73, 2017
Manuscript under review for journal Biogeosciences
Discussion started: 13 March 2017

Figure 2: a) N_2O concentration in surface waters along the cruise track of JR260B. b) N_2O saturations calculated from measured atmospheric and seawater dry mole fractions. Approximate position of Subantarctic Front (SAF) and Polar Front (PF) indicated, based on sea surface temperature and salinity measurements during JR260B.

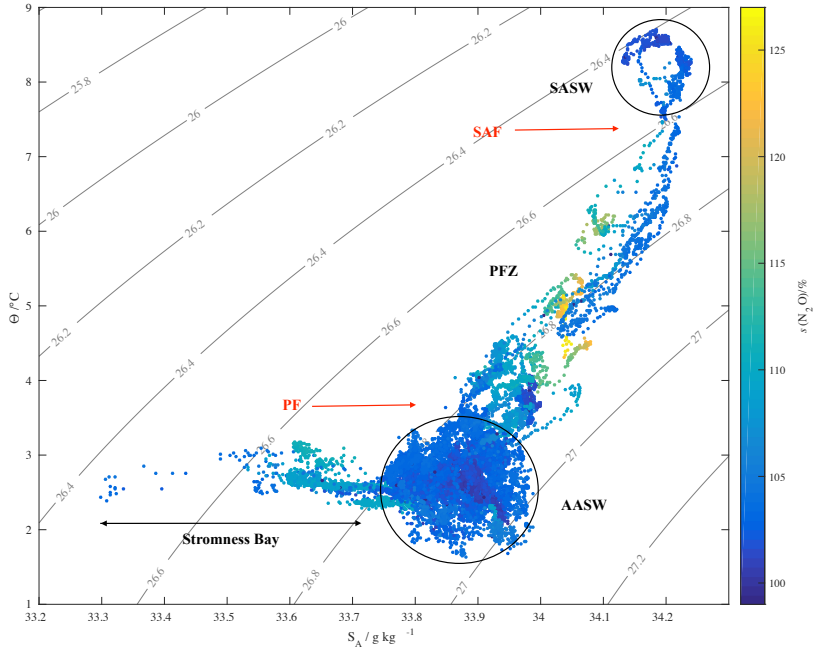

Figure 3: N_2O saturations $s(N_2O)$ with corresponding absolute salinities S_A and conservative temperatures Θ for JR260B. Contour lines are the potential density anomalies (σ_θ) calculated using the TEOS-10 GSW toolbox. Approximate positions of the Subantarctic Front (SAF) and Polar Front (PF) based on sea surface temperature and salinity measurements during JR260B are indicated by red arrows. SASW: Subantarctic Surface Water, AASW: Antarctic Surface Water.

Biogeosciences Discuss., doi:10.5194/bg-2017-73, 2017
Manuscript under review for journal Biogeosciences
Discussion started: 13 March 2017

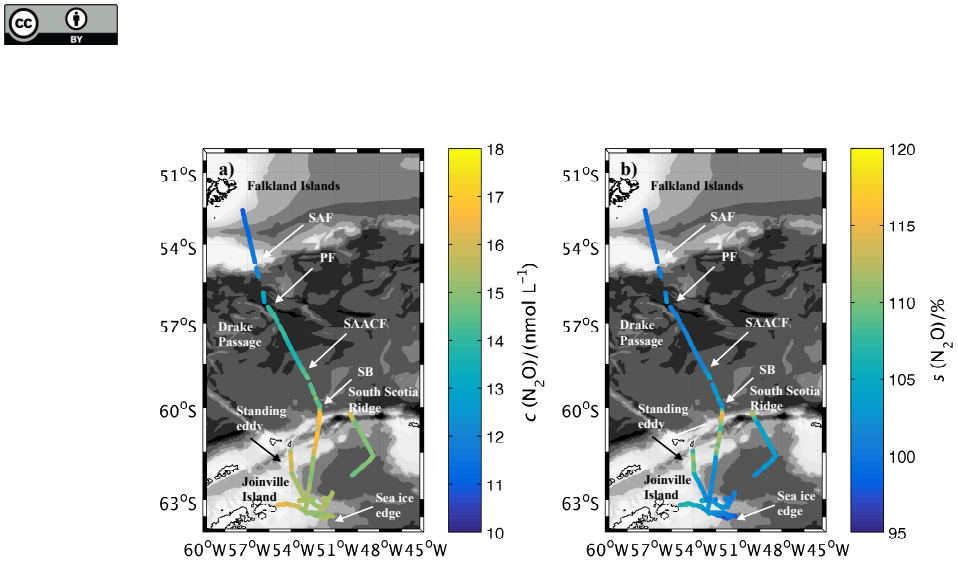

Figure 4: a) N_2O concentrations in surface waters during JR255A/GENTOO. b) Saturations, calculated measured atmospheric and seawater dry mole fractions. Approximate positions of the Subantarctic Front (SAF), Polar Front (PF), Southern Antarctic Circumpolar Current Front (SACCF) and Southern Boundary of the Antarctic Circumpolar Current Front (SACCF) and Southern Boundary of the Antarctic Circumpolar Current (SB) based on sea surface temperature and salinity measurements during JR255A.

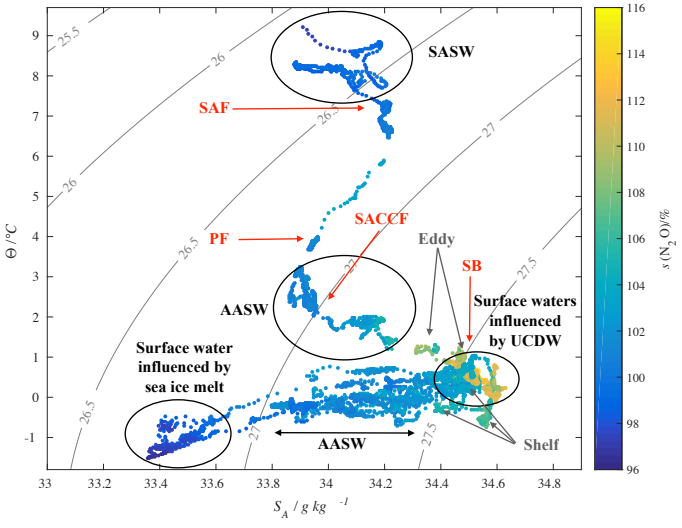

Figure 5: N_2O saturations $s(N_2O)$ with corresponding absolute salinities S_A and conservative temperatures Θ for JR255A/GENTOO. Contour lines are the potential density anomalies calculated using the TEOS-10 GSW toolbox. Approximate positions of the Subantarctic Front (SAF), Polar Front (PF), Southern Antarctic Circumpolar Front (SACCF) and Southern Boundary of the Antarctic Circumpolar

Biogeosciences Discuss., doi:10.5194/bg-2017-73, 2017
Manuscript under review for journal Biogeosciences
Discussion started: 13 March 2017

Current (SB) based on sea surface temperature and salinity measurements during JR255A are indicated by red arrows. SASW: Subantarctic Surface Water, AASW: Antarctic Surface Water, UCDW: Upper Circumpolar Deep Water.

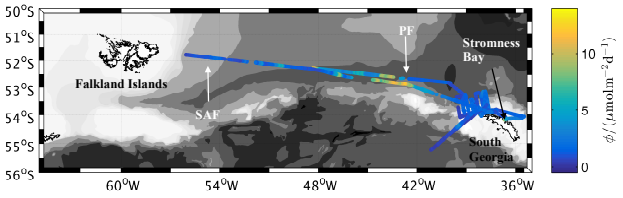

Figure 6: Sea-to-air flux along the cruise track of JR260B. Approximate positions of the Subantarctic Front (SAF) and Polar Front (PF) based on sea surface temperature and salinity measurements during JR260B.

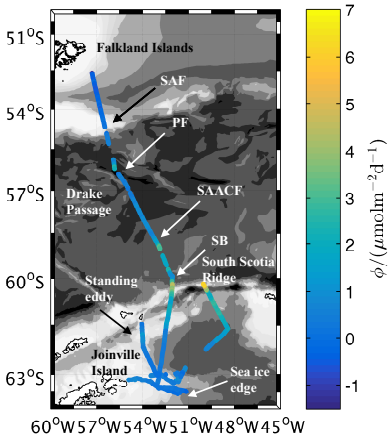

Figure 7: Sea-to-air flux along the cruise track of JR255A. Approximate positions of the Subantarctic Front (SAF), Polar Front (PF), Southern Antarctic Circumpolar Front (SACCF) and Southern Boundary of the Antarctic Circumpolar Current (SB) based on sea surface temperature and salinity measurements during JR255A.